



This is a repository copy of *IoT and machine learning for in-situ process control using Laser Based Additive Manufacturing (LBAM) case study*.

White Rose Research Online URL for this paper:
<https://eprints.whiterose.ac.uk/182646/>

Version: Published Version

Proceedings Paper:

Miller, D. orcid.org/0000-0003-3409-2735, Song, B., Farnsworth, M. et al. (4 more authors) (2021) IoT and machine learning for in-situ process control using Laser Based Additive Manufacturing (LBAM) case study. In: Mourtzis, D., (ed.) *Procedia CIRP. CIRP CMS 2021 - 54th CIRP Conference on Manufacturing Systems, 22-24 Sep 2021, Virtual conference*. Elsevier BV , pp. 1813-1818.

<https://doi.org/10.1016/j.procir.2021.11.306>

Reuse

This article is distributed under the terms of the Creative Commons Attribution-NonCommercial-NoDerivs (CC BY-NC-ND) licence. This licence only allows you to download this work and share it with others as long as you credit the authors, but you can't change the article in any way or use it commercially. More information and the full terms of the licence here: <https://creativecommons.org/licenses/>

Takedown

If you consider content in White Rose Research Online to be in breach of UK law, please notify us by emailing eprints@whiterose.ac.uk including the URL of the record and the reason for the withdrawal request.



eprints@whiterose.ac.uk
<https://eprints.whiterose.ac.uk/>

54th CIRP Conference on Manufacturing Systems

IoT and Machine learning for in-situ process control using Laser Based Additive Manufacturing (LBAM) case study

David Miller^a, Boyang Song^{a,*}, Michael Farnsworth^a, Divya Tiwari^a, Felicity Freeman^b, Iain Todd^b, Ashutosh Tiwari^a

^aDepartment of Automatic Control and Systems Engineering, University of Sheffield, Mappin Street, Sheffield, S1 3JD, United Kingdom

^bDepartment of Materials Science and Engineering, University of Sheffield, Mappin Street, Sheffield, S1 3JD, United Kingdom

Abstract

Additive manufacturing (AM) is emerging within many industrial applications due to inherent advantages such as rapid prototyping and production. However, the correlation of process parameters across modules and their impacts on product quality are not yet fully understood. This article presents a system built out of Internet of Things (IoT) and edge computing technologies to collect and analyze AM process in-situ. An IoT thermal camera platform was developed, and integrated within an Laser Based Additive Manufacturing (LBAM) system to collect information that could be used to characterize the thermal distribution surrounding the melt pool. Machine learning techniques were utilised to identify the occurrence of defects using the collected low-resolution thermal images.

© 2021 The Authors. Published by Elsevier B.V.

This is an open access article under the CC BY-NC-ND license (<https://creativecommons.org/licenses/by-nc-nd/4.0>)

Peer-review under responsibility of the scientific committee of the 54th CIRP Conference on Manufacturing System

Keywords: IoT; Image Processing; Machine Learning; Thermal Imaging

1. Introduction: Research motivation

Additive Manufacturing (AM) is a manufacturing process whereby complex structures are built through the layering of heated materials. This differs from traditional machining techniques which involve subtracting from a block of material to form a shape and offer several advantages such as ease of customisation, minimum use of material, reduced delivery time and maximum flexibility [10]. It has applications in many industries including automotive, aerospace and medicine [20]. Laser Based Additive Manufacturing (LBAM) uses lasers to melt metal alloy powder to form a structure. Despite continuous technological improvements in LBAM systems, process stability and product quality are still affected by several parameters such as laser power, power distribution, scanning velocity, material feed rate, hatch spacing and substrate preheat temperature [6]. This leads to the formation of defects that affect the quality and mechanical performance such as porosity and residual

stress of the structure [11]. As such, there is a keen interest in collecting information that can be used to better understand the process and generation of defects. As the defects occur within structure of the product, one of the main challenges is the selection of appropriate sensing technologies that can adequately perceive them. One approach is to integrate costly industrial-grade sensors to capture the process information. An alternative solution before committing to a defined framework is to integrate low cost sensors to evaluate their efficacy for in-situ control and monitoring. Additionally low cost sensors can accelerate the prototyping process for feasibility research. Furthermore, the environment is hazardous to electronics due to the high temperatures induced by the laser and a significant amount of metal powder getting sprayed into the nearby area. This makes it more cost-effective to prototype using cheaper sensors and test whether it is possible to perceive the target variable.

2. Related work: In-situ control for AM process using IoT & Machine Learning

The advent of Industry 4.0 has driven the need for manufacturers to collect more information and gain a better understand-

* Corresponding author

E-mail address: b.song@sheffield.ac.uk (Boyang Song).

ing of their shop floor. The current trend is to connect devices into a network commonly referred to as an Internet of Things (IoT) [15]. This network of distributed devices helps to fill in knowledge gaps about the current state of the factory leading to better allocation of resources and a more optimised process [17].

Several IoT platforms have been developed and implemented in an industrial setting. Wang et. al. proposed a cloud based system that manages the information collected from a series of networked AM machines and allows customers to submit manufacturing requests directly to the machines. The information collected includes test data, design files, and machine status information [20]. Barbosa et al. attached a Bluetooth beacon to several AM machines to collect and broadcast information to mobile devices handled by managers and operator [8]. When device users approach connected machines, the application displays machine information without the need for inspection. Trabesinger et al. collected information using an industrial device called SINUMERIK Edge to collect, process and send information via the internet making it easily accessible to other members of the office with access to the network [19].

Machine Learning (ML) is a class of algorithms with the ability to learn from experience to improve performance or make predictions [13]. Li et al. created a predictive model using machine learning that combines multiple sensor sources to estimate the surface roughness of extrusion-based additive manufacturing [12]. Zhu et al. combined a prescriptive deviation modelling method with machine learning techniques to predict deviations in additive manufacturing [21]. Caggiano et al. trained a Deep Convolutional Neural Network architecture that accepts images from two different sources to detect patterns indicative of a defect [4]. Baturynska et al. proposes a conceptual optimisation framework combining machine learning and finite element modelling to identify the best process parameters for powder bed fusion additive manufacturing [1].

3. Methods and instruments

Methods. A key feature of additive manufacturing is the melt pool. This is the channel formed when a pulse of power from the laser combines with the powder to form part of the product's structure. The size and depth of the melt pool is influenced by the power of the laser and the type of material being used. As it forms the structure, the mechanical properties of the melt pool once cooled should be captured to detect whether it becomes a potential point of failure [16]. Recently Khanzadeh et al have proposed a methodology for using thermal imaging and modelling of the melt pool to understand and model the characteristics of porosity during LBAM [9]. This work proposes an IoT based setup that comprises of a thermal camera to achieve in-situ process control during an LBAM process. The camera records information about subsurface temperature distribution and this information is then processed utilising ML techniques to detect defects in the structure.

Instruments. The camera chosen is the Adafruit MLX90640 thermal camera. The camera can sense from -40 to 400 °C and

is sensitive to changes of 1 °C. The camera was chosen as it was designed to connect with the popular Raspberry Pi edge computing platform and the manufacturer supplying an open source software library for handling the retrieval of temperature values. The library handles the low-level interactions including the required physics calculations so the user can directly retrieve the temperature values with minimum hassle. The camera is recorded by the edge computing platform Raspberry Pi Model 3B+. This platform was chosen for its ability to interact with a wide range of sensors and devices. The platform runs an instance of the Linux operating system making it a flexible environment for developing in a range of programming languages. The camera is connected to the platform by a Breakout Garden breakout board designed so that the camera can be inserted without soldering wires onto the camera thus simplifying maintenance and making it easier to use. Figure 1a shows how the components are connected to each other and 1b shows the platform's housing.

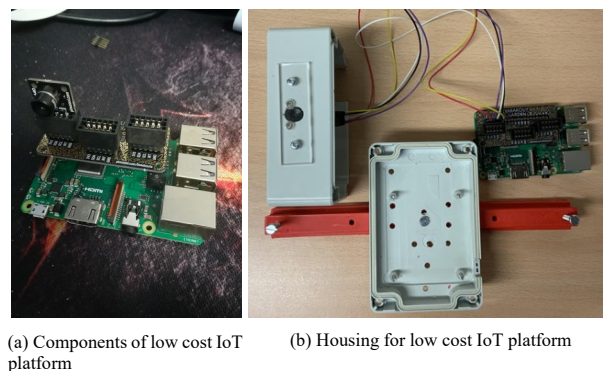


Fig. 1. Contents of the thermal camera platform

Use case: BeAM machine. The BeAM Magic 2.0 machine based at The University of Sheffield, is a blown powder, direct energy deposition (DED) AM machine [2]. It comprises of a laser head which is moveable along five degrees of freedom and is managed by a separate motor controller. The position, velocity and electrical current history of the motor is recorded. The laser supply can transmit a laser with a maximum of 500 Watts with the power set and triggered by the machine's central controller. A thermal camera was installed connected in parallel with the laser head and provides a fixed view point of the build site. The camera records the radiative heat from the build site and is started with a trigger signal sent from the central controller.

The building process takes place within an air tight chamber inside the machine designed to prevent metal powder from escaping to the outside. This chamber can be observed through a window on one side of the machine and a port hole on the door to the chamber. The products are built on a titanium build plate which is fixed in the centre of the chamber on top of a metal circle with four channels spaced at equal angles. A custom slot liner was 3D printed that was designed to fit in one of these channels. It had a series of screw holes added along the length of the beam where the thermal camera platform could be

mounted at a fixed distance and angle relative to the build site. Figure 2 shows the thermal camera platform fitted inside the BeAM machine while it was in use. For the arrow shape build, the camera platform was setup at a distance of 15 cm.

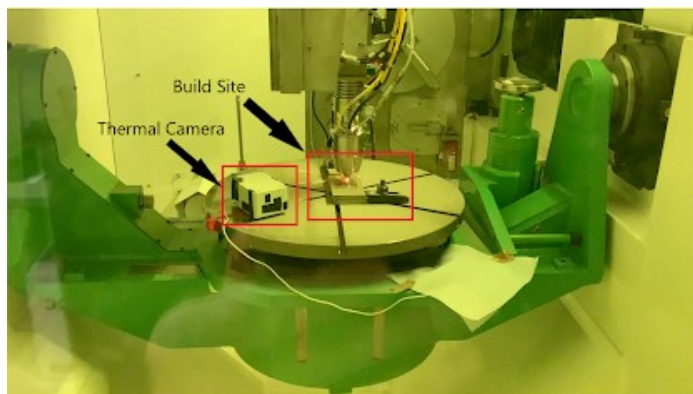


Fig. 2. Developed thermal camera platform in-use inside the BeAM machine

4. Results and Discussion

Two builds were conducted to collect data using our developed thermal camera platform. The first build was a complex arrow shape and the second was three parallel lines at a fixed distance from each other. The arrow shape build yielded the most interesting data and will be the focus of this paper. Figure 3 shows the laser head position history recorded by the motor controller during the build collectors afterwards. Stainless Steel 314L was used for fabricating the selected shape. The shape is made up of four layers each composed of the same structural components; an arrow head and three rectangles forming the tail.

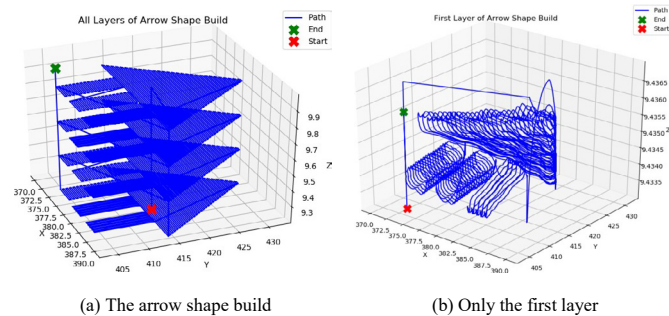


Fig. 3: Position history of the laser head

The thermal camera was able to collect data with some distinct dynamics. Figure 4a shows the maximum temperature of each camera frame. The recording software was set to record to capture for three hours in order to capture the temperature before the build, the build period and the cooling period afterwards. The two clear spikes in the graph were confirmed to be data errors as they are far outside of the camera sensing range. The activity between frames 90000 and 150000 is the period of time where the product was being built. Figure 4b shows a region of the plot assumed to be associated with the arrow head section.

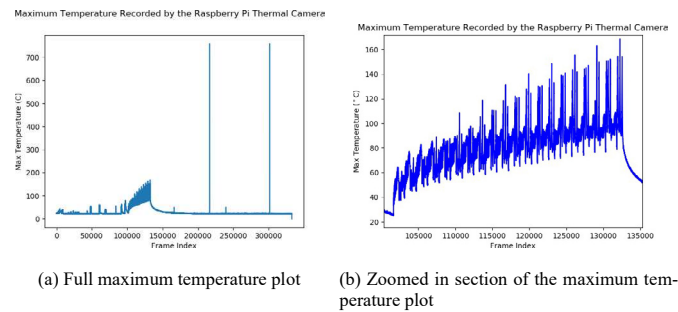


Fig. 4. Maximum temperature of each frame recorded by the developed thermal camera platform during the arrow shape build

Figure 5a shows examples of the data collected by the developed thermal camera platform (24x32 image) during the arrow shape build. Units of x and y axis are pixels. The colorbar represents temperature in °C. All of the frames contain a distinct T-shape similar to the one showed. The component along the plot y-axis is the path of the laser from the laser head to the build plate and ends at the temperature peak. The component taking up most of the x-axis is the sub-surface heat distribution during the build. This is the most important section of the data as it contains the information relating to the formation of the melt pool. The amount of detail that can be captured from this experimental setup depends on how close the laser is to the camera. Overall, the data captured shows that the temperature distribution drops off sharply at the boundary (approx. 20-30 °C) of the sub-surface heat distribution limiting the effective sensing range.

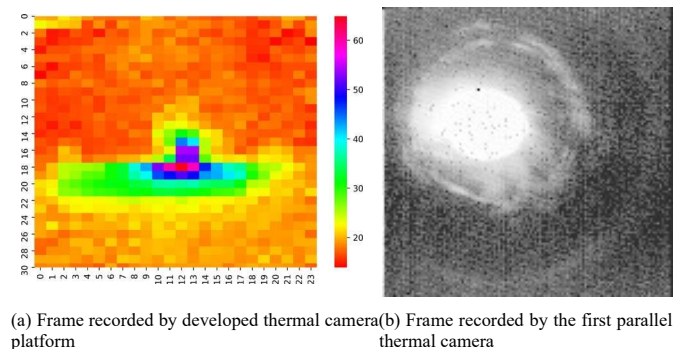


Fig. 5. Examples of the thermal camera footage recorded during the arrow shape build

Figure 5b shows an example of the footage recorded during the arrow shape build using the first parallel thermal camera. This camera captured an off-centre view of the laser surface power distribution over the build site. The data is displayed in grayscale with the white pixels representing the higher values. The image captured has a distinct circular boundary defining the process region.

Surface laser power can be estimated by converting the recorded radiative heat to laser power density. An approximated model was developed to convert pixel wise heat to pixel wise temperature and then to laser power density. The material's thermal response parameters, such as thermal diffusivity and

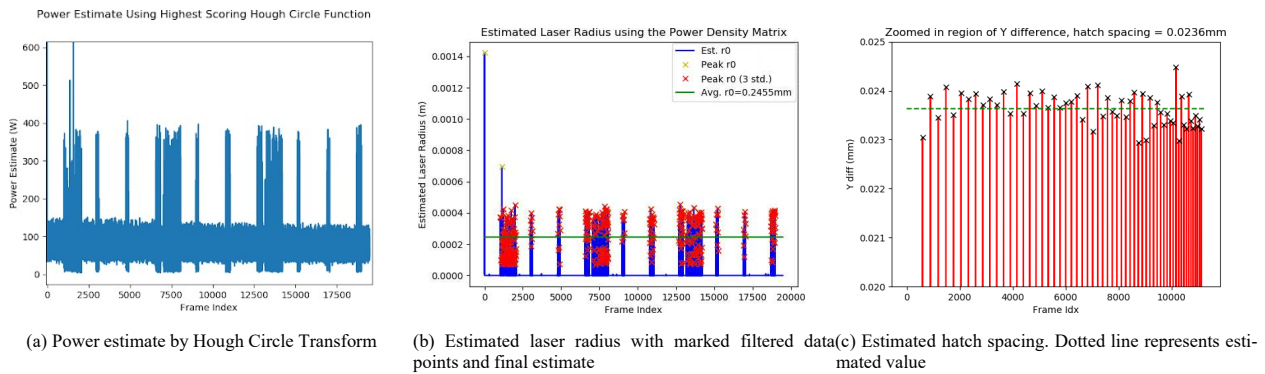


Fig. 6. Estimated hatch spacing. Dotted line represents estimated value

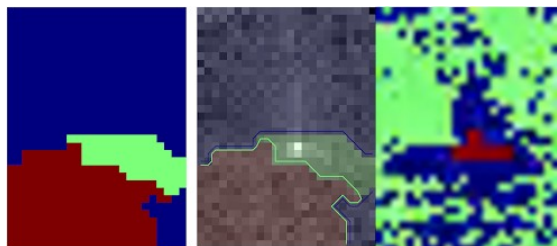
conductivity, were estimated from several datasheets. As these parameters were for specific temperature ranges, a function was fitted to interpolate in between the ranges. To estimate power the heating boundary needs to be identified. The Hough gradient method [14] was applied as the heating area can be seen to be predominately circular. Figure 6a shows the power estimate results using the highest scoring circle according to the algorithm¹. As it's an image processing technique, each frame had to be normalised and converted to a grayscale image. The maximum estimate of the laser power under this method was 400 Watts which when compared to the target of 500 Watts was reasonably close. This data was going to produce an underestimate as the thermal camera records the surface radiative heat and does not record the subsurface temperature. Furthermore when the laser is inactive, the conversion to an image weights the noise highly due to the rescaling being based off the local maximum which may cause the transform to detect falsely large or small circles resulting in an incorrect estimate.

One process parameter that can be estimated from the first parallel camera's thermal footage is the laser radius. A common approach is the $1/e^2$ method which measures the maximum distance between two points in the laser power density where the intensity has fallen to $1/e^2$ times the peak value. Figure 6c shows the estimated laser radius using this method and the post-processing steps to improve the result. The peaks in the dataset were identified and abnormal values more than three standard deviations of the mean were filtered. The spike at the start of the file is caused by a single frame in the footage where all the values are the maximum for the datatype. The cause for this is unknown. The laser radius is taken as the average of the filtered data resulting in a value of 0.2454 millimetres. The target laser radius is 0.35 millimetres. The difference can be attributed to the post processing technique erroneously filtering beyond noise in the image and the recorded emitted heat values not being representative of the true heat at the build site. One of the most important process parameters in LBAM is hatch spacing. It is the distance between the tracks built by the laser head that form the build layers. Studies have shown that it affects the

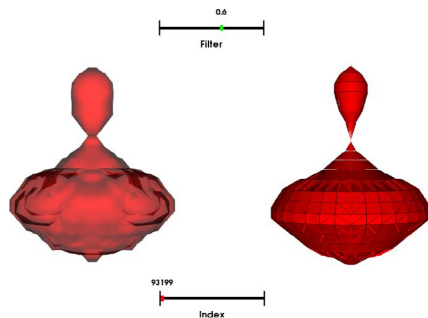
heat transfer behaviours, surface quality and overlap rates [7]. Increasing the hatch spacing decreases the build time but results in pockets of unmelted powder to form affecting the build structure and high porosity. The hatch spacing can be estimated from the laser head position by looking at the element wise distance between the y-position values. Figure ?? shows a region of the distance values with the dotted line indicating an average hatch spacing of 0.0236 millimetres. The difference between the estimate and the target is believed to be due to the quality of the control system.

One of the objectives with any manufacturing system is fewer defects in the product. By seeing how the temperature distributes below the surface it may be possible to detect the formation of defects. Unsupervised machine learning is a class of machine learning algorithms that attempts to separate the data into groups based on its parameters and has been shown to be effective in anomaly detection [18]. Figure 7a shows examples of the results from two trialled methods. Both were set to classify the regions into three classes containing the background (blue), foreground (green) and defect (red) respectively and each frame was treated independently. Figure 7a is a result from using a pre-built unsupervised segmentation pipeline. Originally developed by Borovec et al. for clustering regions of medical images into active and inactive ones, the multistage pipeline classifies regions based on their colour and texture features [3]. The pipeline was able to consistently separate the thermal activity from the background and the labels remaining stable with only a couple of occasions when the activity labels swapped identities. The background label also consistently contained minimal noise resulting in reasonably clean and contained boundaries. The non-background labels repeatedly separated the surface activity initially induced by the laser and the sub-surface activity that emanates from it. Figure 7a shows an example of applying k-means clustering. Like with the pipeline, it was able to separate the thermal activity from the background with reasonable success but noise was repeatedly misclassified as non-background. One solution is to use information from previous frames to stabilise the classification of future frames.

¹ The Hough Circle transform searches a parameter space of possible circle centres and radii. Each circle is given a vote for every non-zero pixel that fits within the equation that describes the circle creating an accumulated score.



(a) Unsupervised learning results from pre-built pipeline (left and middle) and K-means clustering (right)



(b) Early attempt at 3D modelling using Gaussian Splat (left) and Delaunay Triangulation (right).

Fig. 7. Unsupervised clustering of thermal images using a pre-built pipeline and K-Means clustering

This work opens an avenue of research to attempt to model a more realistic 3D representation of the sub-surface heat distribution. Figure 7b shows an early attempt to represent power density around and including the melt pool, visualised in a 3D model. This was done using Gaussian Splat and Delaunay Triangulation [5]. These methods were investigated to roughly estimate the volume of the melt pool as a possible metric for the quality of the build. Further details on the experiment and the computational pipeline can be found in the repository referenced in the Supplementary Material.

5. Conclusion

In this paper, an IoT-grade thermal camera was used to monitor the thermal distribution through a melt pool. This work demonstrated that it can detect the heat distribution region of interest including features suitable for further processing (3D modelling of the heat distribution containing the melt pool). The process data was characterised using unsupervised machine learning techniques in an attempt to identify defects. This reinforces the case for cheap IoT technology being a valid way to monitor manufacturing processes. One of the biggest limitations with controlling AM processes is the lack of understanding about the impact of process parameters on build quality. The data collected by this project's AM machine was used to estimate important parameters such as hatch spacing, laser radius and laser power. These estimates and a better understanding of the key data features will help to outline an in-process framework that will help improve process repeatably and stability. These results help justify the integration of the low cost sensors to supplement existing industrial systems for in-process control and monitoring.

Acknowledgements

The work reported here was sponsored by Research England's Connecting Capability Fund award CCF18-7157 – Promoting the Internet of Things via Collaboration between HEIs and Industry (Pitch-In). The authors would like to acknowledge the support of Airbus and the Royal Academy of Engineering (REA1718/1/20, RCSRF1718/5/41) under the Research Chairs and Senior Research Fellowships scheme.

References

- [1] Baturynska, I., Semeniuta, O., Martinsen, K., 2018. Optimization of Process Parameters for Powder Bed Fusion Additive Manufacturing by Combination of Machine Learning and Finite Element Method: A Conceptual Framework. *Procedia CIRP* 67, 227–232. doi:10.1016/j.procir.2017.12.204.
- [2] BEAM, 2020. BEAM 2.0 Product details. URL: <https://www.beam-machines.com/products/magic800>.
- [3] Borovec, J., Švihlík, J., Kybic, J., Habart, D., 2017. Supervised and unsupervised segmentation using superpixels, model estimation, and graph cut. *Journal of Electronic Imaging* 26, 1. doi:10.1117/1.JEI.26.6.061610.
- [4] Caggiano, A., Zhang, J., Alfieri, V., Caiazzo, F., Gao, R., Teti, R., 2019. Machine learning-based image processing for on-line defect recognition in additive manufacturing. *CIRP Annals* 68, 451–454. doi:10.1016/j.cirp.2019.03.021.
- [5] Chen, L., Xu, J., 2004. Optimal delaunay triangulations. *Journal of Computational Mathematics*, 299–308.
- [6] DebRoy, T., Zhang, W., Turner, J., Babu, S., 2017. Building digital twins of 3D printing machines. *Scripta Materialia* 135, 119–124. doi:10.1016/j.scriptamat.2016.12.005.
- [7] Dong, Z., Liu, Y., Wen, W., Ge, J., Liang, J., 2018. Effect of hatch spacing on melt pool and as-built quality during selective laser melting of stainless steel: Modeling and experimental approaches. *Materials* 12. doi:10.3390/ma12010050.
- [8] GF, B., RV, A., 2017. An IoT-Based Solution for Control and Monitoring of Additive Manufacturing Processes. *Journal of Powder Metallurgy & Mining* 06, 1–7. doi:10.4172/2168-9806.1000158.
- [9] Khanzadeh, M., Chowdhury, S., Bian, L., Tschopp, M.A., 2017. A methodology for predicting porosity from thermal imaging of melt pools in additive manufacturing thin wall sections. *ASME 2017 12th International Manufacturing Science and Engineering Conference, MSEC 2017 collocated with the JSME/ASME 2017 6th International Conference on Materials and Processing 2*, 1–10. doi:10.1115/MSEC2017-2909.
- [10] Khorram Niaki, M., Nonino, F., 2017. Additive manufacturing management: a review and future research agenda. *International Journal of Production Research* 55, 1419–1439. doi:10.1080/00207543.2016.1229064.
- [11] Kim, F.H., Moylan, S.P., 2018. Literature Review of Metal Additive Manufacturing Defects. *NIST Advanced Manufacturing Series*, 100–116doi:10.6028/NIST.AMS.100-16.
- [12] Li, Z., Zhang, Z., Shi, J., Wu, D., 2019. Prediction of surface roughness in extrusion-based additive manufacturing with machine learning. *Robotics and Computer-Integrated Manufacturing* 57, 488–495. doi:10.1016/j.rcim.2019.01.004.
- [13] Mohri, M., Rostamizadeh, A., Talwalkar, A., 2018. *Foundations of Machine Learning*, second edition. Adaptive Computation and Machine Learning series, MIT Press.
- [14] OpenCV, 2019. OpenCV Hough Circle Transform. URL: https://docs.opencv.org/master/d4/d70/tutorial_hough_circle.html.
- [15] Patel, K.K., Patel, S.M., Scholar, P.G., 2016. Internet of Things-IOT: Definition, Characteristics, Architecture, Enabling Technologies, Application & Future Challenges. *International Journal of Engineering Science and Computing* 6, 1–10. doi:10.4010/2016.1482.
- [16] Reutzel, E.W., Nassar, A.R., 2015. A survey of sensing and control systems for machine and process monitoring of directed-energy, metal-

- based additive manufacturing. *Rapid Prototyping Journal* 21, 159–167. doi:[10.1108/RPJ-12-2014-0177](https://doi.org/10.1108/RPJ-12-2014-0177).
- [17] Rong, W., Vanan, G.T., Phillips, M., 2017. The internet of things (IoT) and transformation of the smart factory. *Proceedings - 2016 International Electronics Symposium, IES 2016*, 399–402. doi:[10.1109/ELECSYM.2016.7861039](https://doi.org/10.1109/ELECSYM.2016.7861039).
- [18] Saadia Razvi, Sayyeda; Feng, Shaw; Narayanan, Anantha; Tina Lee, Yung-Tsun; Witherell, P., 2019. A Review of Machine Learning Applications in Additive Manufacturing. *Proceedings of the ASME 2019 International Design Engineering Technical Conferences and Computers and Information in Engineering Conference*.
- [19] Trabesinger, S., Butzerin, A., Schall, D., Pichler, R., 2020. Analysis of High Frequency Data of a Machine Tool via Edge Computing. *Procedia Manufacturing* 45, 343–348. doi:[10.1016/j.promfg.2020.04.028](https://doi.org/10.1016/j.promfg.2020.04.028).
- [20] Wang, Y., Lin, Y., Zhong, R.Y., Xu, X., 2019. IoT-enabled cloud-based additive manufacturing platform to support rapid product development. *International Journal of Production Research* 57, 3975–3991. doi:[10.1080/00207543.2018.1516905](https://doi.org/10.1080/00207543.2018.1516905).
- [21] Zhu, Z., Anwer, N., Huang, Q., Mathieu, L., 2018. Machine learning in tolerancing for additive manufacturing. *CIRP Annals* 67, 157–160. doi:[10.1016/j.cirp.2018.04.119](https://doi.org/10.1016/j.cirp.2018.04.119).